Operation of a free electron laser from the extreme ultraviolet to the water window

by W. Ackermann et al.

Supplementary Information

1 Introduction

In the early 90s, the TESLA Test Facility (TTF) was established by the international TESLA collaboration as a test bed for studies of superconducting linac technology for a future linear collider [1]. To this end, work at TTF was focused on achieving an accelerating gradient around 25 MV/m and on the development of techniques to manufacture such accelerating components in a reliable and cost-effective way. Furthermore, experimental verification of the components performance in terms of field quality, beam dynamics, reliability, diagnostics tools and control procedures was a key objective.

It was realized very soon, that a superconducting accelerator like TTF would be perfectly suited to drive a free-electron laser (FEL) at wavelengths far below the visible [2], mainly for the following reasons:

- Due to the large iris diameter of the accelerator cavities, wake field effects, eventually degrading the electron beam quality, are very small compared to standard normal conducting cavities.
- Due to its excellent power efficiency, a superconducting linac can be operated at very high duty cycle, up to continous wave operation, a fact that allows for very high average brilliance and for large flexibility in terms of timing structure.

Based on these superior properties, the vision from the very beginning was to develop superconducting FEL technology in a manner which permitted operation across a large range of wavelengths, down to the X-ray regime [3, 4]. As a first step in the realization of an XFEL, a wavelength around 100 nm (unreacheable at that time with conventional lasers) was chosen as a target value. The TTF accelerator was upgraded by adding a laser-driven rf gun, a bunch compressor, and

Figure S1: Aerial view of the experimental hall for the FLASH User Facility in Hamburg (center) and the tunnel for the superconducting accelerator and undulator (covered with grass). The hall in the upper right corner houses the injector section of the linac. The total length of the FLASH facility is 300 meters. The maximum energy of electrons is 1 GeV, and the minimum radiation wavelength is 6 nm.

a 15 m long undulator. This installation, called TTF FEL, Phase1, successfully reached its design goals in 2001 [5, 6]. This success has become a triggering event for the launch of big XFEL projects: the European X-ray FEL and LCLS [7, 8].

In a second phase, the scientifically attractive VUV wavelength range between 6 nm and 60 nm was targetted. The superconducting linac was upgraded to 700 MeV beam energy, an additional bunch compressor and a 30 m long undulator was installed, and a hall for user experiments was built. This facility, now called FLASH, has been in operation for users since August, 2005 (see Fig. S1). Currently the minimum wavelength (around 13 nm) is limitetd by energy of electrons. After the energy upgrade of the FLASH linac to 1 GeV planned in 2007, it will be possible to generate wavelengths down to 6 nm.

Table 1: Parameters of FLASH

	FLASH-2006	Design
Electron beam		
Energy, MeV	700	1000
Peak current, kA	1.5-2.5	2.5
Emittance, norm., mm-mrad	1-2	2
# of bunches/train	600	7200
bunch train length, ms	0.6	0.8
Rep. rate, Hz	5	10
Undulator		
Period, cm	2.73	
Gap, mm	12	
Peak magnetic Field, T	0.48	
Undulator parameter K (rms)	0.87	
total length, m	27.3	
FEL radiation		
Wavelength, nm	13-47	6-60
Average pulse energy, μJ	100	500
Pulse duration (fwhm), fs	10-50	200
Peak power, GW	3	2-3
Average power, W	0.1	10-20

2 Description of FLASH facility

The main elements of free-electron laser FLASH are a laser-driven rf gun, superconducting accelerator with bunch compressors and an undulator (see Fig. 1 in the paper). FLASH operates in pulsed mode with a 'macropulse' repetition rate of up to 5 Hz. Each macropulse is 0.8 ms long. Within each macropulse FLASH generates up to 800 micropulses separated by 1 μs. A brief description of FLASH subsystems is given in [9].

2.1 Laser-driven rf gun

Both small emittance values and high phase space densities in all three dimensions are mandatory for development of the FEL amplification process. Since in a linac no radiative damping occurs and the emittance generally tends to increase (e.g.

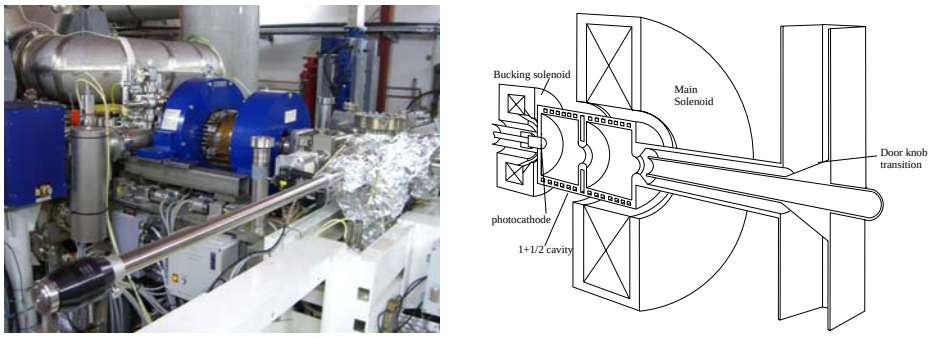

Figure S2: Left: view of rf gun in the FLASH tunnel. Right: cross sectional view of the RF gun along with the main and bucking solenoid and the RF input coupler.

due to collective force within the bunch), the electron bunches have to be produced by the gun with an emittance smaller than that specified in the undulator. The development of a RF-gun based on photo-emission [10] allows the production of such high phase space density beams.

The injector of FLASH places tight constraints on the electron beam quality for XFELs [11] (see Fig. S2). The rf gun and a laser system have been successfully tested and optimized at the PITZ injector test stand at Zeuthen and installed at the FLASH facility in January 2004 [12]. It is a 1.5 cell, normal cunducting L-band cavity (1.3 GHz, TM_{010} mode) powered by a 5 MW klystron. A longitudinal coupler is used to keep the cylindrical symmetry around the beam axis as close to perfect as possible. The RF gun is operated with an rf power of 3MW (41MV/m on the cathode) and an RF pulse length of up to 0.9 ms. A low level RF system based on digital signal processors reads the forward and reflected power from the gun and regulates the RF power and RF phase in the gun by acting on the low level RF input to the klystron with a vector modulator. The phase stability achieved lies below 0.2 degrees and the amplitude stability Is confined to within 0.1% [13].

A Cs_2Te photocathode is inserted into the RF gun backplane via a load-lock system and can be changed if required. The cathode quantum efficiency achieved (for UV light) is initially high (more than 5%) and drops to a level of 1% after months of usage [14]. The laser is based on a pulsed mode-locked pulse train oscillator synchronized to the 1.3 GHz RF of the accelerator [15]. The phase stability is better than 0.5 ps. A chain of linear Nd:YLF amplifiers provides sufficient laser pulse energy to convert the initial infrared wavelength into the UV with a single pulse (262 nm) energy of about 1 μJ required for extraction of the

Table 2: Parameters on the photoinjector laser

Wavelength	262 nm
Energy on photocathode/bunch	~ 1 μJ
Train rep. rate	10 Hz
Pulse train length (max.)	800μs
Number of bunches per train (max.)	7200
Pulse spacing (min.)	111 ns

charge of a few nC from a photocathode. The system produces pulse trains with up to 800 s length at a repetition rate of up to 10 Hz. The pulse spacing is usually 1 μs (1 MHz), a 9 MHz mode is in preparation. The charge fluctuation of a single electron bunch from shot to shot is better than 2% rms, if averaged over a train, it is better than 1%. The rms pulse length in the UV measured with a streak camera is 4.4 ± 0.1 ps.

2.2 Superconducting accelerator

The five accelerator modules (each 12.2 m in length) comprise the main body of the linac [16] (see Fig. S3). Each module contains eight TESLA type 9-cell cavities operated in standing-wave π-mode, a superconducting quadrupole / steerer package, and a cold cavity type beam position monitor. Each accelerating structure has one input coupler for RF power, and a small pickup antenna to measure the cavity field and amplitude. Two higher order mode couplers provide sufficient damping. A frequency tuning mechanism is used to operate the cavities on resonance. In the standard linac configuration two accelerating modules (16 cavities) are driven by one klystron. The maximum accelerating gradient in the best cavities is 35 MV/m. The average gradient is about 22 MV/m. With five accelerating modules the maximum energy of the FLASH linac is about 700 MeV.

The low level RF system provides field control for the superconducting cavities with the vector-sum of cavity groups (up to 16 cavities in each group). Presently controlled are 1 cryomodule before the bunch compressor and 4 cryomodules in the linac. The most challenging field requirements are for the cryomodule (8 cavities) before the bunch compressor where the first 4 cavities are operated at 12 MV/m and the last four cavities at 20 MV/m. This section is operated 10 degrees off-crest to provide the necessary beam energy chirp for the bunch compression. The requirements here are 2×10^{-4} for amplitude and 0.03 degree for phase.

Figure S3: Superconducting accelerator of FLASH. Yellow barrels are superconducting modules with accelerating gradient up to 25 MV/m.

This stability has been verified for short bunch trains [17]. The stability depends critically on the precision of the calibration of the vector-sum which is based on transient beam loading.

Exception detection and handling in the superconducting cavities includes cavity quench and recovery from interlock trips. Basic automation schemes have been implemented for loop phase, loop gain, cavity detuning and loaded Q measurement as well as fault recovery. These features allow for high availability which has been demonstrated during long term user operation.

The main limitation in the Low Level RF (LLRF) system are long term phase drifts from the frequency distribution system which will be upgraded in the near future. The phase drift are corrected by beam based feedback to ensure the required long term stability.

The essential goal for the FEL is high peak current, small emittances, small momentum spread, and short bunch length. Also, any energy chirp along the bunch should not be too large in order to prevent degradation of the FEL gain and an increase of the width of the photon spectrum. The FLASH linac incorporates a two stage magnetic compression scheme. The first magnetic compressor, 4-bend chicane [18], is located at the energy of approximately 130 MeV, in the injector area. The second stage compression occurs downstream of the third accelerating module at the energy of 380 MeV. The chicane chosen is a S-type chicane [19] optimized to have a minimum emittance dilution due to coherent synchrotron ra-

diation. As a consequence of the bunch length being a non negligible fraction of the rf wavelength of 23 cm, the particle distribution in the longitudinal phase space (momentum vs. longitudinal position in the bunch) acquires an rf-induced momentum variation during the acceleration. This energy-position correlation is then used for tailoring the bunch shape in the bunch compressors. In these chicanes, electrons with larger momentum travel a shorter distance than electrons with smaller momentum thus enabling the bunch tail to catch up with the head of the bunch if the appropriate longitudinal momentum profile is imprinted to the bunch. The longitudinal electron distribution inside the bunch consists of a 20-50 fs long leading spike with current exceeding 1 kA and a long tail with current too small as to expect significant FEL gain. The evolution of the electron beam in the accelerator depends on the accelerating electric fields and the magnetic guide fields, both acting on each electron independently, and on collective forces such as space charge fields and coherent synchrotron radiation.

After acceleration to the final energy the electron beam passed through the collimation section. A collimation section protects the undulators from radiation due to off-energy and off-orbit particles. The design includes two copper collimators in the straight and two in a dogleg section allowing, in addition, collimation of off-energy particles. The energy acceptance of the collimator is $\pm 3\%$.

2.3 Undulator

Single pass high gain FELs require long undulator systems. The FLASH undulator system consists of six modules with a length of 4.5 m each [20] (see Fig. S4). Each undulator utilises permanent NdFeB magnets. With a fixed gap of 12 mm, the peak magnetic field is 0.48 T while the undulator period is 27.3 mm. A pair of electromagnetic quadrupoles, located between each of the six modules, provides a large acceptance in beam energy. In terms of FEL radiation it covers the wavelength range of 120 to 6 nm. Each quadrupole doublet is aligned on a stable granite base plate together with beam position monitors and a vertical and horizontal wirescanner. The absolute alignment, with respect to the undulator axis, is better than 100 μm. The SASE process requires an alignment of the electron beam with the undulator axis of better than 20 μm. Therefore, the quadrupoles are equipped with moveable stages allowing a fine adjustment of their position.

Figure S4: Undulator of FLASH is a permanent magnet device (period 2.73 cm, gap 12 mm, peak field 0.48 T). The undulator system is subdivided into six segments, each 4.5 m long. The vacuum chamber has 9 mm inner diameter.

3 Electron beam diagnostics

The linac includes a large variety of diagnostic tools to measure the transverse and longitudinal beam properties, bunch positions, current etc. [21]. The diagnostics are essential for controlling and characterizing the lasing process. Many new systems had to be designed for the very short, high intensity electron beam pulses at FLASH. Most diagnostic devices have been commissioned and are routinely used during machine operation and some are included in feedback systems, such as the bunch compression monitors. Other systems are used occasionally to understand and correct the beam, e.g., in emittance measurements. Novel diagnostics are continually designed and tested during machine study periods.

3.1 Measurements of the beam charge

In addition to the Faraday cup in the gun region, the charge is measured by toroids [21]. These use the wall current transformer principle and provide a single bunch resolution of 0.5%. The cavity BPMs also provide the bunch charge [22, 23].

3.2 Measurements of the beam position

Beam position monitors (BPM) of various kinds are built in all along the accelerator [24, 25, 22, 23]. They have the capability to monitor each bunch in a pulse of typically 1 MHz repetition frequency. Most other BPMs in the linac show a resolution better than 10 μm rms. The BPMs in the undulator section [24] show a single-bunch resolution of about 20 μm rms at this time. So called higher order mode BPMs are currently being tested for monitoring the beam position within all 40 accelerating cavities [26, 27]. They monitor one resonant mode excited by the beam in these cavities.

3.3 Beam loss monitors

The FLASH linac can currently be operated with a beam power of up to 2.8 kW. Future upgrades will increase the beam energy as well as the repetition rates of micro- and macropulses, raising this figure to approximately 72 kW. To protect the accelerator and surrounding equipment from direct damage and from induced activation, beam losses are monitored by a set of 18 secondary emission multipliers and 63 photomultiplier/scintillator combinations distributed along the machine. These beam loss monitors detect charge losses of a few pC, and serve as inputs to the machine protection system [28, 29].

3.4 Measurements of the beam energy

Spectrometer The total electron beam energy gained on the passage through the linac is measured with beam position monitors installed in a spectrometer section upstream the undulator. A server provides on line constant monitoring of the beam energy with relative energy resolution of $dE/E < 2 \cdot 10^{-4}$ [30].

Large aperture BPM A BPM with a large horizontal aperture, based on striplines, set perpendicular to the beam direction, has recently been installed in the first bunch compressor. By precise measurement of the beam position with an electro-optical modulator phase measurement technique, the jitter of the energy can be monitored. An improved bunch-to-bunch energy resolution of less than $dE/E < 5 \cdot 10^{-5}$ is expected [31] to be achieved. First beam tests have promising results.

Synchrotron radiation A synchrotron radiation camera was installed at the third dipole of the first bunch compressor to monitor the energy profile of the

dispersed bunches. This camera records the emitted SR in the visible part of the spectrum. This system was successfully tested and is being commissioned [32].

3.5 Measurements of the beam phase

Two different systems measure the bunch arrival time, at specific fixed locations of the beamline, with respect to a reference signal. Both methods use broadband beam pick-ups with a bandwidth of several GHz.

Time-of-Flight monitor In the first approach, the pick-up signal is filtered by a narrowband filter with a center frequency at the reference frequency of 1.3 GHz. This signal is mixed with the reference oscillation using the mixer as phase detector. The difference in bunch arrival times for pairs of beamline locations, the Time-of-Flight (TOF), is then calculated in order to eliminate the effect of varying charge per bunch. The purpose of this system is the determination of the on-crest phase and the optimization of the bunch compression process. To fulfill these requirements, the TOF is measured between beamline sections with energy-dependent trajectory lengths, i.e. bunch compressors, for various phases of the RF field in the accelerating cavities. In this way, the dependence of the compression process on the accelerating field is determined [33]. This will be even more important, when the third harmonic cavity is built in [34].

Bunch arrival monitor A second scheme [35] is based on the upcoming laser based synchronisation system in which ultra-short laser pulses are distributed via stabilized fiber links to the components to be synchronized. For the arrival time detection, these pulses are fed into an electro-optical modulator which uses the beam pick-up signal as the modulation voltage. In this way, a change in the bunch arrival time is converted into a laser amplitude change, which can be detected by a photo-detector and sampled by a fast ADC. Since the synchronization system is used directly, no additional timing jitter is added. The resolution of the current system is 20-30 fs. A resolution below 10 fs seems feasible.

3.6 Control of longitudinal bunch profile

Several new instrumentation techniques are used for measuring the longitudinal profile of the short bunches.

Bunch compression monitors The compression of the electron bunches is monitored using infrared-sensitive pyroelectric detectors that register the coherent radiation intensity emitted in the form of synchrotron-, transition or diffraction radiation. The total intensity increases with a shortening of the bunch [36], and can thus be used to stabilize the longitudinal charge distribution. Two such bunch compression monitors are installed after both bunch compressors, one registering synchrotron radiation from the last dipole, and other registering diffraction or transition radiation from a radiator station. The phase of the first accelerating module is adjusted regularly during user operation in a feedback loop that keeps the signal from a downstream compression monitor constant.

More advanced compression monitors, based on spectrally resolving the radiation, are studied at a dedicated experimental station further downstream of the accelerator [37]. This uses wavelength dependent diffracting devices and multichannel sensors to measure the signal in different wavelength channels simultaneously. Changes in the radiation spectrum indicate changes in the longitudinal structure of the bunch.

LOLA cavity An S-band transverse deflecting cavity (LOLA) [38] with a length of 3.66 m was installed just before the collimator section. This cavity can streak one electron bunch out of the bunch train and project it onto an off-axis screen, where the longitudinal profile is measured [39]. LOLA is also being used for measurement of the slice emittance and the slice energy spread [40].

Electro-optical devices The LOLA cavity has the disadvantage that it does not allow the operator to non-distructively monitor multiple bunches in a macro-pulse train. Therefore, two non-disruptive electro-optical (EO) devices are used to parasitically monitor multiple bunches in a macro-pulse [41, 42]. One of them uses a diagnostic laser synchronized to the machine RF. The longitudinal beam profile is encoded in the intensity profile of a chirped laser pulse, whose spectrum is then analyzed. The second system uses a Titanium-Sapphire-based laser system. In this case the electron bunch profile is encoded into a spatial dimension of the laser by an intersection angle between the laser and the electron beam at the EO crystal. With these systems, single-shot longitudinal bunch profiles can be measured. The jitter of the bunch arrival time can also be monitored.

3.7 Emittance measurements

The transverse electron beam distribution (shape and size) is measured by optical transition radiation (OTR) monitors. Optical transition radiation is visible light generated when an electron beam passes through a boundary between two media of different optical properties, in our case a silicon wafer with an aluminum coating. This radiation is imaged by a camera system providing on-line images of the electron beam as well as information of the beam shape and size for off-line analysis. Seven of the 25 OTR monitors are combined with a wirescanner providing a complementary measurement of the electron beam size. Along the undulator the electron beam size is measured using wirescanners only. The transverse projected emittance, an important parameter characterizing the quality of an electron beam, is determined from simultaneous measurements of the transverse beam distribution at four or more locations along the beam line with well-defined beam optics. At the FLASH injector, with an electron beam energy of 127 MeV, normalized projected rms emittances below 2 mm mrad for a 1 nC uncompressed bunch have been measured. Details of the emittance measurements, results, and error analysis are in [43].

4 Photon diagnostics

The photon beam diagnostic section is located in the FEL beam line to measure the properties of the FEL radiation. An overview of the various tools is given in [44, 45]. An important instrument for tuning the onset of laser amplification and optimizing the lasing is a detector based on gold wires and a micro-channel plate (MCP) [46]. The dynamic range of this detector is sufficient to cover several orders of magnitude of radiation energy, from spontaneous (a few tens of nJ) to the saturation level (about 100 μJ). The detector has been carefully calibrated; its relative accuracy is of the order of 1%. Since the wire produces unwanted diffraction resulting in an inhomogeneous intensity distribution at the sample position, this device is not suitable for online monitoring of the intensity while operating with user experiments.

Thus, for user operation two gas-monitor-detectors [47, 48] are in routine operation at FLASH, measuring the photon flux in a non-destructive way. These devices are absolutely calibrated monitor detectors based on photoionisation of gases at low target density. Ions and electrons created in the interaction volume are extracted and accelerated in opposite directions by a homogeneous electric

field. They are detected by simple Faraday cups, in order to avoid saturation of any amplifying particle detector due to the great number of secondary particles in the range of 10^6 to 10^9 created during one single FEL radiation pulse.

The extended dynamic range of the gas-monitor detector guarantees, on the one hand high linearity, even in the saturation regime, of the non-focused FEL beam, and allows on the other hand, its calibration using dispersed synchrotron radiation at low photon intensities. The standard relative uncertainties of about 10% for the measured photon numbers per FEL radiation pulse are dominated by the inherent statistical fluctuations of the FEL-pulse intensities.

View screens using Ce:YAG crystals are placed at various locations which are used to control spatial profile and position of the photon beam.

Three monochromators were used to measure radiation spectra. A high resolution monochromator is installed in the accelerator tunnel and is used for measurement of single shot spectra. It is equipped with an intensified CCD camera and has a resolution of 0.02 nm with an absolute calibration error of less than 0.03 nm.

The monochromator beamline at FLASH is designed as a plane grating monochromator with an SX700 mount described in detail by Martins et al. [49]. The beamline can be used not only as a versatile tool for spectroscopy, but also as a high resolution spectrometer itself. Therefore, by moving the exit slit, a CeYAG crystal can be steered into the dispersed beam path in the exit slit plane to monitor the individual SASE spectra. The system is equipped with a gated fast shutter ICCD allowing one to record the image of any pulse within a bunchtrain. The monochromator has a spectral resolution of 10,000 to 70,000 depending on the cff value and the grating. The system is equipped with a high transmission 200 grooves/mm grating and a high resolution 1200 grooves/mm grating. At present the resolution of the recorded spectra is not limited by the mirrors and grating of the beamline, but by the optics of the ICCD camera and the fluorescence screen to about one seventh of the theoretical value. For a cff value of 1.5 and the 200 grooves/mm grating we obtain a total transmission of about 20% for the fundamental at 90 eV while for the second and third harmonic at 180 eV and 270 eV we obtain 30% and 35%, respectively, yielding enough fluorescence on the CeYAG crystal to be monitored by the ICCD. All optical components of the beamline are covered with DLC coatings to withstand the high power of the FEL radiation. Therefore, the transmission drops down to 1-2% above the carbon edge.

5 SASE tuning and measurements of the radiation energy

FLASH is equipped with a set of detectors for measurements of the energy in the radiation pulse: gas monitor detector [48], MCP-detectormcp-detector, photodiode, and thermopile [44]. The detectors are installed in several positions along photon beam line. The distance of the nearest detector unit is 18.5 m downstream of the undulator exit. The most critical step of tuning lasing process is to find the signature of light amplification. The problem relates to a strong background of incoherent radiation produced by the whole bunch (charge 0.5-0.7 nC) passing through the whole undulator length(27 m). In the present experimental conditions, the pulse energy of spontaneous emission is about 40 nJ within the 10 mm aperture of the detector located 18.5 m downstream of the undulator. Thus, it becomes crucial to have high-precision photon detectors permitting the detection of small increases in the radiation intensity. For this purpose a radiation detector equipped with a microchannel plate (MCP) was used, which features a dynamic range of seven orders of magnitude and allows coverage of the entire range of intensities from spontaneous emission up to FEL saturation [46]. The MCP measures the radiation scattered by a gold mesh (wire diameter 60 μm, open window 250×250 μm) placed behind a 10 mm aperture located 18.5 m downstream of the undulator. The electronics of the MCP-detector itself has low noise, about 1 mV at a level of signal of 100 mV (1% relative measurement accuracy). Another source of disturbances of measurements were fluctuations of the bunch charge. To exclude the influence of bunch charge fluctuations we performed on-line normalization of the radiation energy to the bunch charge. This technique gave us the possibility to detect reliably SASE gain at a 2% level above spontaneous emission. Once amplification is detected, output energy can be easily increased to the level of about ten μJ, the onset of the saturation regime. This occurs due to the exponential dependence of the output signal on a change in any important parameter of the electron beam. Tuning of the radiation energy in the saturation regime above 10 μJ is a delicate procedure, and requires perfect alignment of the orbit in the undulator (on a scale of ten micrometers), and the rf phases of the gun and the first three accelerating modules with relative accuracy of about 0.1 degree.

Once the SASE process is optimized over the whole undulator length, we perform measurements of the gain curve as it is described in the paper, and measurements of statistical properties. We should note that a special experimental procedure was applied to guarantee that statistical distributions represent fundamental

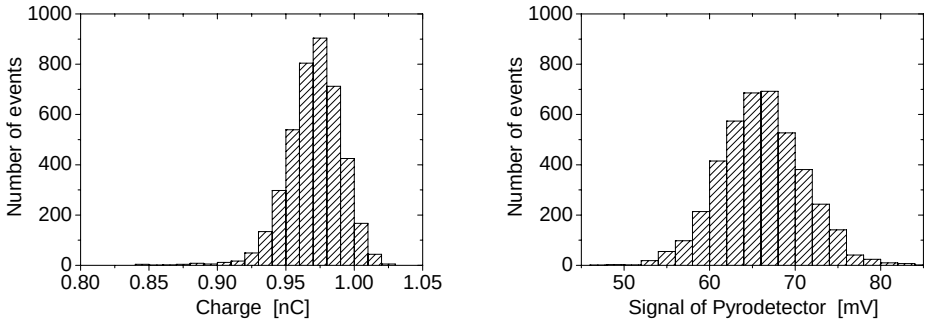

Figure S5: Probability distributions of row data for the charge monitor and pyrodetector (left and right plot, respectively.)

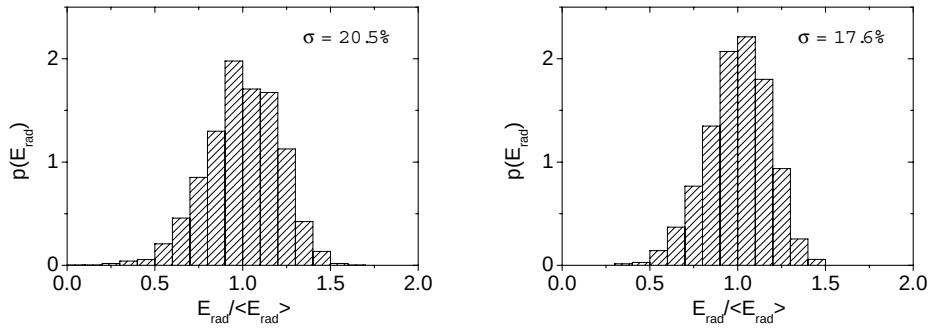

Figure S6: Illustration of machine fluctuations and fundamental fluctuations due to start-up from shot noise. Left plot: probability distribution of row data. Right plot: probability distribution for the shots filtered via gate on pyrodetector ($\pm 4\%$) and charge monitor ($\pm 4\%$).

SASE fluctuations, but not machine fluctuations. For each shot we recorded the radiation energy together with the main parameters of the electron bunch which relate directly to the FEL process: charge and pyrodetector (see Fig. S5. Then we gated experimental data for the radiation energy such that those events for which the deviation of charge or pyrodetector signal from nominal values were larger than some threshold were excluded. Figure S6 illustrates relative contribution of the machine fluctuations. The left plot in this figure shows raw data while the right plot shows data gated with a $\pm 3\%$ deviation for the charge, and a $\pm 4\%$ deviation for pyrodetector signal. After such a gating of the experimental results we obtain perfect agreement with theoretical predictions as it is shown in Fig. 4 of the paper.

6 Statistical properties of the radiation filtered through narrow bandwidth monochromator

An important subject is statistics of the SASE FEL radiation filtered through a narrow-band monochromator. In the linear stage of SASE FEL operation the value of normalized energy deviation is equal to unity and energy fluctuates in accordance with a negative exponential distribution:

$$p(E) = \exp\left(-\frac{E}{\langle E \rangle}\right) . \tag{1}$$

This is consequence of the fact that the radiation from a SASE FEL operating in the linear regime is a random process described by gaussian statistics [50, 51]. This property remains valid for any pulse length. When the amplification process enters the nonlinear stage the SASE FEL radiation is no longer a gaussian random process due to the growth of sidebands in the nonlinear media. In particular, the probability distribution of the total radiation energy does not follow agamma distribution anymore as one can see from Fig. 4 in the paper. The situation with the probability distribution of the radiation energy filtered by a narrow band monochromator is more complicated. Earlier studies have shown that in the case of a long radiation pulse (much longer than coherence length) the property of the negative exponential distribution remains to be valid in the nonlinear regime as well [50, 51]. However, the situation changes dramatically when pulse duration is reduced to a timescale on the order of one coherence length. Recent studies have shown that in this case strong suppression of the fluctuations of the radiation energy after narrow band monochromator is expected [52]. Subsequently this effect was measured experimentally at the VUV FEL, phase I [5, 6]. Experimental results presented in Fig. S7 demonstrate such a suppression as well. This effect has a simple physical explanation [52]. Let us consider an extreme case of SASE FEL driven by an electron bunch of about a coherence length. For this extreme case each radiation pulse consists of a single spike only. For different shots the radiation pulses have a similar shape, but their amplitude fluctuates nearly according to a negative exponential distribution. When the amplification process enters the nonlinear regime, the amplitudes of different pulses are equalized due to saturation effects, while maintain the original shapes. The spectrum of the radiation pulse is given by the Fourier transform of the radiation field, and at saturation we obtain a nearly similar spectral envelope for different pulses. As a result, we can expect that fluctuations in the radiation energy after a narrow-band monochroma-

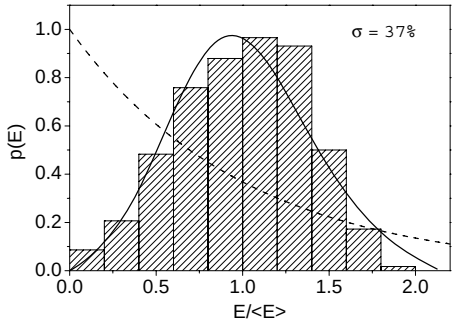

Figure S7: Probability distribution of the energy in the radiation pulse having passed through a narrow band monochromator. Average energy in the radiation pulse is 40 μJ. Radiation wavelength is 13.7 nm. Solid line represents the probability distribution simulated with code FAST [53]. Dashed line shows a negative exponential distribution (1) which corresponds to the case of a long photon pulse.

tor should follow fluctuations of the total energy in the radiation pulse which drop drastically (see Fig. 4 in the paper). For longer radiation pulses suppression is not so strong and nearly vanishes for bunches longer than four coherence lengths. Thus, the measured suppression of fluctuations of the radiation energy following passage through a narrow band monochromator is a clear signature of an ultrashort radiation pulse, of about one coherence length.

References

[1] Edwards, D.A. (Ed.). TESLA Test Facility Linac - Design Report. TESLA 95-01 (1995).

[2] Aberg, T. et al. A VUV FEL at the TESLA Test Facility at DESY. TESLA-FEL 95-03 (1995).

[3] Brinkmann, R. et al. (Eds.). Conceptual Design of 500 GeV e^+e^- Linear Collider with Integrated X-ray Facility. DESY 1997-048, ECFA 1997-182 (1997).

[4] Richard, F. et al. (Eds.). TESLA Technical Design Report. DESY 2001-11, ECFA 2001-209, TESLA Report 2001-23, TESLA-FEL 2001-05 (2001).

[5] Ayvazyan, V, et al. Generation of GW radiation pulses from a VUV free-electron laser operating in the femtosecond regime. Phys. Rev. Lett. **88**, 104802 (2002).

[6] Ayvazyan, V, et al. A new powerful source for coherent VUV radiation: Demonstration of exponential growth and saturation at the TTF free-electron laser. Eur. Phys. J. D **20**, 149-156 (2002).

[7] Altarelli, M. et al. (Eds.): XFEL: The European X-Ray Free-Electron Laser. Technical Design Report. Preprint DESY 2006-097, DESY, Hamburg, 2006 (see also http://xfel.desy.de).

[8] Arthur, J. et al. Linac Coherent Light Source (LCLS). Conceptual Design Report. SLAC- R593, Stanford, 2002 (see also (http://www-ssrl.slac.stanford.edu/lcls/cdr).

[9] Ayvazyan, V, et al. First operation of a free-electron laser generating GW power radiation at 32 nm wavelength. Eur. Phys. J. D **37**, 297-303 (2006).

[10] Fraser, J., & Sheffield, R. A new high-brightness electron injector for free electron lasers driven by RF linacs. Nucl. Instr. Meth. **A285**, 71-76 (1986).

[11] Schreiber, S. Commissioning of the VUV-FEL Injector at TTF. Proc. EPAC 2004 Conference (Lucerne, Switzerland) p.351-353 (2004).

[12] Krasilnikov M. et al. Optimizing the PITZ Electron Source for the VUV-FEL. Proc. EPAC 2004 Conference p. 360-362 (Lucerne, Switzerland, 2004).

[13] Vogel, E., Koprek, V. & Pucyk, P. FPGA-based rf field control at the photocathode rf gun of the DESY VUV-FEL. Proc. 2006 Eur. Part. Acc. Conf., Edinburg, Scotland, p.1456-1458.

[14] Sertore, D. et al. irst operation of cesium telluride photocathodes in the TTF injector RF gun. Nucl. Instr. Meth. **A445**, 422-426 (2000).

[15] Will, I., Liero, A., Mertins, D. & Sandner, W. Feedback-stabilized Nd:YLF amplifier system for generation ofpicosecond pulse trains of an exactly rectangular envelope. IEEE Journ. Quan. Electronics **34**, 2020-2028 (1998).

[16] Weise, H. Superconducting rf structures - test facilities and results. Proc. 2003 Part. Acc. Conf., p. 673-677.

[17] Ayvazyan, V. et al. Bunch-to-bunch energy stability test of the Nb prototypes of the TESLA superstructure. Proc. 2003 Part. Acc. Conf., p. 2730-2732.

[18] Limberg, T., Piot, Ph. & Stulle, F. Design and performance simulation of the TTF-FEL II bunch compression system. Proc. EPAC 2002 Conference,p. 811-813 (2002).

[19] Loulergue, A. & Mosnier, A. A simple S-chicane for the final bunch compressor of TTF-FEL. Proceedings EPAC2000 Vienna, 752-754 (2000).

[20] Pfluger, J. Undulators for SASE FELs. Nucl. Instrum. and Methods **A445**, 366-372 (2000).

[21] Nölle, D. The diagnostic system of TTF II. Proc. EPAC 2002, Paris, France, 242-244 (2002).

[22] Lorenz, R. First operating experinece of beam position monitors in the TESLA Test Facility linac. Proc. PAC97, Vancouver, Canada, 1997, pp.2137-2139 (1997).

[23] Simon, C. et al. High resolution BPM for linear colliders. Proc. BIW 2006, Batavia, IL, U.S.A., 2006.

[24] Nölle, D. & Wendt, M. BPMs with precise alignment for TTF2. Proc. LINAC 2004, Lübeck, Germany, 2004, pp. 435-437 (2004).

[25] Baboi, N. et al. Resolution studies at beam position monitors at the FLASH facility at DESY. Proc. BIW 2006, Batavia, IL, U.S.A., 2006.

[26] Molloy, S. et al. High precision superconducting cavity diagnostics with higher order mode measurements. Phys. Rev. ST Accel. Beams **9**, 112802 (2006).

[27] Molloy, S. et al. Using higher order modes in superconducting accelerating cavities for beam monitoring. Proc. Linac 2006, Knoxville, TN, U.S.A., 2006.

[28] Fröhlich, L. et al. First operation of the FLASH machine protection system with long bunch trains. Proc. Linac 2006, Knoxville, TN, U.S.A., 2006.

[29] Nölle, D. et al. The beam inhibit system for TTF II. Proc. DIPAC2003, Mainz, Germany, 2003.

[30] Hacker, K. et al. TTF2 ACC5 Gradient Measurement. DESY-TESLA-FEL-NOTES-2005-09 (2005).

[31] Hacker, K. et al. BPM with large horizontal aperture. Proc. EPAC 2006, Edinburgh, Scotland, 2006.

[32] Gerth, Ch. On-line energy spectrum measurements using synchrotron radiation in the bunch compressors at FLASH. Proc. FEL 2006, Berlin, Germany, 2006.

[33] Kollewe, M. & Flöttmann, K. Applications of time-of-flight measurements at FLASH. Proc. Linac 2006, Knoxville, TN, U.S.A., 2006.

[34] Solyak, N. et al. Development of the third harmonic SC cavity at Fermilab. Proc. PAC 2003, Portland, OR, U.S.A., 2003.

[35] Löhl F. et al. A sub 100 fs electron bunch arrival-time monitor system for FLASH. Proc. EPAC 2006, Edinburgh, Scotland, 2006.

[36] Grimm O. & Schmüser, P. Principles of longitudinal beam diagnostics with coherent radiation. TESLA FEL 2006-03 (2006).

[37] Delsim-Hashemi, H. et al. Bunch compression monitor. Proc. EPAC 2006, Edinburgh, Scotland, 2006.

[38] Akre, R. et al. Bunch deflecting measurements using a transverse rf deflecting structure in the SLAC linac. Proc. EPAC 2002, Paris, France, 2002

[39] Hüning, M. et al. Observation of femtosecond bunch length using a transverse deflecting structure. Proc. FEL 2005, Stanford, CA, U.S.A., 2005.

[40] Röhrs, M. et al. Energy-time correlation measurements using a vertically deflecting rf structure. Proc. EPAC 2006, Edinburgh, Scotland, 2006.

[41] Steffen, B. et al. Single shot longitudinal bunch profile measurements at FLASH using electro-optic techniques. Proc. EPAC 2006, Edinburg, Scotland, 2006.

[42] Schlarb, H. et al. Comparative study of bunch length and arrival time measurements at FLASH. Proc. EPAC 2006, Edinburgh, Scotland, 2006.

[43] Loehl, F. et al. Measurements of the transverse emittance at the FLASH injector at DESY. Phys. Rev. ST Accel. Beams 9, 092802 (2006).

[44] Treusch, R. Photon Diagnostics for the VUV-FEL. HASYLAB Annual Report, DESY, Hamburg, 2005, p.159-164 (see also http://www-hasylab.desy.de/science/annual_reports/2005_report/index.html).

[45] Tiedtke, K. et al. The SASE FEL at DESY: photon beam diagnostics for the user facility. AIP Conf. Proc. **705**, 588-592 (2004).

[46] Bytchkov, A. et al. Development of MCP-based photon diagnostics at the TESLA Test Facility at DESY. Nucl. Instrum. and Methods A **528**, 254-257 (2004).

[47] Richter, M. et al. Verfahren und Monitordetektor zur Bestimmung der Intensitat von gepulster VUV- oder EUV-Strahlung sowie Verwendung eines derartigen Monitordetektors (Deutsches Patent- und Markenamt, No. 102 44 303.3, Munchen)(2002).

[48] Richter, M. et al. Measurement of gigawatt radiation pulses from a vacuum and extreme ultraviolet free-electron laser. Appl. Phys. Lett. **83**, 2970-2972 (2003).

[49] Martins, M. et al. Monochromator beamline for FLASH. Rev. Sci. Instr. **77**, 115108 (2006).

[50] Saldin, E.L., Schneidmiller, E.A. & Yurkov, M.V. *The physics of free electron lasers* (Springer-Verlag, Berlin, 1999).

[51] Saldin, E.L., Schneidmiller, E.A. & Yurkov, M.V. Opt. Commun. **148**, 383-403 (1998).

[52] Saldin, E.L., Schneidmiller, E.A. & Yurkov, M.V. Statistical properties of radiation from SASE FEL driven by short electron bunches. Nucl. Instrum. and Methods **A507**, 101-105 (2003).

[53] Saldin, E.L., Schneidmiller, E.A. & Yurkov, M.V. FAST: a three-dimensional time-dependent FEL simulation code. Nucl. Instr. Meth. A **429**, 233-237 (1999).